scientific reports

Check for updates

OPEN

Synthesis, characterization, antioxidant and antimicrobial activities, and computational studies of chitosan nanoparticles loaded with vitamin E and clove essential oil

Davoud Mahmoudi[1], Abolghasem Abbasi Kajani[1]✉ & Mohammad Rabbani Khorasgani[2]

Efficient encapsulation of bioactive compounds in the food-grade delivery systems to improve their stability, efficiency, and bioavailability and to develop functional foods is a novel and interesting field of research in food industry. Here, two unstable and hydrophobic food ingredients including vitamin E (Vit E) and clove essential oil (CEO) were encapsulated in the chitosan nanoparticles (ChNPs) by the emulsion/ ionic gelation technique without using any toxic surfactant. The physicochemical characterization by DLS, FTIR, FE-SEM, and TEM, confirmed the synthesis of high colloidal and monodispersed ChNPs with narrow size distribution of less than 50 nm. MTT assay showed high biocompatibility of ChNPs after CEO loading, with the increased cellular viability of 72.84% for CEO loaded ChNPs. ABTS and DPPH assays also revealed high antioxidant activity of CEO loaded ChNPs with maximum activity of 75.66%. Co-loading of Vit E and CEO led to the antioxidant activity of 77.7% over 48 h, potent antibacterial effect on *E. coli* and *S. aureus* with the inhibition zone diameters of 14–17 mm, and complete growth inhibition of fungus *A. niger*. Molecular docking studies also showed strong binding of chitosan, eugenol, and α-tocopherol to different bacterial and fungal proteins. Overall results indicated that Vit E and CEO loaded ChNPs represent interesting physicochemical and biological properties and high potential for development of food preservatives and functional foods.

Keywords Chitosan nanoparticles, Vitamin E, Clove essential oil, Antibacterial, Antioxidant

Abbreviations

3D	Three-dimensional
A. niger	*Aspergillusniger*
ChNPs	Chitosan nanoparticles
DLS	Dynamic Light Scattering
DPPH	1,1-Diphenyl-2-picrylhydrazyl
EO	Essential oil
FTIR	Fourier Transform Infrared Spectroscopy
MBC	Minimum Bactericidal Concentration
MTT	3-(4,5-Dimethylthiazol-2-yl)-2,5-diphenyltetrazolium bromide
OD	Optical density
PBP	Penicillin Binding Proteins
PDB	Protein data bank
TEM	Transmission Electron Microscope
UV–Vis	Ultraviolet–visible

[1]Department of Biotechnology, Faculty of Biological Science and Technology, University of Isfahan, Isfahan 81746-73441, Iran. [2]Department of Cell and Molecular Biology and Microbiology, Faculty of Biological Science and Technology, University of Isfahan, Isfahan 81746-73441, Iran. ✉email: agh.abasi@gmail.com; agh.abbasi@bio.ui.ac.ir

ABTS	2,2'-Azino-*bis* (3-ethyl benzothiazoline-6-sulfonic acid)
CEO	Clove essential oil
DHFR	Dihydrofolate reductase
DMSO	Dimethyl sulfoxide
E. coli	*Escherichia coli*
FE-SEM	Field Emission Scanning Electron Microscopy
IZ	Inhibition zone
MIC	Minimum Inhibitory Concentration
NPs	Nanoparticles
PBS	Phosphate Buffered Saline
PDA	Potato Dextrose Agar
SD	Standard deviation
TPP	Tripolyphosphate
Vit E	Vitamin E

Plant essential oils (EOs) with well-known antioxidant and antimicrobial properties have found different applications especially in food, pharmaceutical and perfumery industries[1,2]. However, the high instability, hydrophobicity, and volatile nature of EOs are the main obstacles to their widespread application[3,4]. The volatile components of EOs are prone to decomposition or evaporation under processing in high temperatures or low pressures, and exposure to air and light[5]which significantly reduce their antibacterial and antioxidant activities[6,7]. Therefore, tremendous efforts have been devoted to overcome these limitations and to improve the stability and long-time preservation of EOs[8,9]. The clove (*Syzygium aromaticum*) EO (CEO) is rich in the bioactive phenylpropanoids, including cinnamaldehyde, eugenol, carvacrol, and thymol, with the valuable biological properties[2,5,10]. The antioxidant, antimicrobial, antiseptic, pesticide, analgesic, and anticarcinogenic activities of CEO have been reported and used in the food, sanitation, biomedical, pharmaceutical, active packaging, and cosmetic products[10]. CEO is also used as a natural preservative, colorant, and flavoring agent in various food products[10–12]. However, the hydrophobic and volatile nature of CEO limits its widespread applications. On the other hand, vitamin E (Vit E), a plant-based lipophilic antioxidant consisting of a chromanol ring attached to a long isoprenoid side chain, possess distinct physiological functions and critical role in the normal human growth[13,14]. Although Vit E is frequently used in food industry, the hydrophobicity of Vit E significantly decreases its efficiency[15,16].

Among different methods suggested to increase the stability, shelf life, and biodistribution of bioactive compounds, their encapsulation is considered as an effective and promising approach that also enables their controlled release[17]. Chitosan (Ch) is considered as an excellent candidate for the encapsulation of bioactive compounds, due to the biodegradability and biocompatibility as well as easy chemical modifications via the various functional groups[18]. Moreover, the well-known antimicrobial properties of Ch also enhance its effectiveness as a preservative coating. In this regard, the ionotropic gelation method is greatly considered for Ch encapsulation, due to its simplicity, high efficiency, significant stability, high loading capacity, good water dispersibility, and controlled delivery of bioactive compounds[19]. Different EOs, such as oregano, eugenol, and carvacrol, have been successfully encapsulated using Tripolyphosphate (TPP)-Ch through emulsion-ionic gelation technique[20]. There have been various reports on the loading of Vit E and clove essential oil into Ch. The positive effects of Vit E-loaded Ch nanoparticles (ChNPs) and nanocomposites on the growth performance and innate immune system of Nile tilapia have been reported[21,22]. The viscosity and drying rate of Ch films as well as their solubility and thermal properties were reported to be influenced by the incorporation of Vit E[23]. The nano-emulsions of CEO and oregano EOs incorporated in the Ch edible films have been reported to extend the shelf life of sliced bread[24]. The improved antioxidant and antibacterial activities of CEO-loaded ChNPs have also been reported, recently[25]. Since both CEO and Vit E are hydrophobic and show significant antioxidant activity, their co-loading into a nanoparticle can increase their bioavailability and bioactivity. Moreover, incorporation of CEO and Vit E may affect the physicochemical properties of ChNPs.

To evaluate this hypothesis, we first tried to synthesize high stable colloidal ChNPs using ionotropic gelation method in the presence of CEO and Vit E, without using any chemical emulsifiers that are usually toxic. The physicochemical properties of resulted ChNPs were subsequently characterized and their biocompatibility, antioxidant, antibacterial and antifungal activities were investigated. Finally, the computational (molecular docking) studies were used to reveal their antibacterial mechanism of action. These computational studies were used to further clarify the molecular-level interactions of Ch, eugenol, and α-tocopherol to different bacterial and fungal proteins and to provide mechanistic support for the observed biological effects. To the best of our knowledge, there is no other report on the co-encapsulation of CEO and Vit E in ChNPs and investigation of such different bioactivities. It is anticipated that the results of this study will lead to the development of a new nano-formulation based on natural compounds with various potential applications in the food industry, especially as a preservative. These bioactive compounds can be used as an interesting alternative to the commonly used chemical preservatives.

Materials and methods

Materials

Low molecular weight Ch (50–190 kDa) with 75–85% degree of deacetylation, and TPP (CAS # 7758-29-4; technical grade) were purchased from Sigma-Aldrich (Germany). 2,2'-azino-*bis* (3-ethylbenzothiazoline-6-sulfonic acid) (ABTS), 1,1-diphenyl-2-picrylhydrazyl (DPPH), potassium persulfate, sodium hydroxide, potato dextrose agar (PDA) and Vit E were supplied by Merck (Germany). Two bacterial strains of *Staphylococcus aureus* (*S. aureus*, ATCC25923) and *Escherichia coli* (*E. coli*, ATCC25922), and fungal strain of *Aspergillus niger*

(*A. niger*, ATCC IBRC-M 30095) were prepared from department of microbiology faculty of biology, university of Isfahan (Isfahan, Iran). All other chemicals utilized in this project were of analytical grad. The reference antibiotics of amoxicillin and gentamicin were prepared as a gift from Farabi pharmaceutical Co. (Isfahan, Iran). All aqueous solutions were prepared by double distilled water. The human fibroblast cells were provided from Pasteur Institute of Iran. CEO was prepared by the hydrodistillation of dried and powdered clove buds using a Clevenger, based on the previous method[26].

Synthesis of ChNPs and CEO-Vit E ChNPs

The oil loaded particles were prepared based on the two-step approach of droplet formation and solidification, according to the previous reports[27,28] with some modifications. Briefly, the oil-in-water emulsion was first prepared by the addition of CEO in a Ch solution under ultrasonication (Hielscher UP200S Germany, 70% amplitude) for 15 min at 25 °C. Then, the NPs solidification was carried out through the ionic gelation by the dropwise addition of TPP solution (1% w/v) at pH 4.6 and stirring for 60 min at 25 °C. To obtain the optimum condition, different concentrations of Ch solution (0.25, 0.5, 0.75, 1% w/v) were prepared in the aqueous acetic acid solution (1%, v/v) under stirring at 25 °C, overnight. The resulted NPs were then collected by the centrifugation at 9000 × g for 15 min at 4 °C and subsequent washing with deionized water. The samples were immediately freeze dried (Cryodos 50/230 V, Telstar, Madrid, Spain) at −32 °C for 42 h and dry weight of NPs was measured to find the optimum mass ratio of Ch to TPP. The effect of different mass ratios of Ch to CEO (0.5:1.3, 0.5:2.6, 0.5:3.9, 0.5:5.2), Ch to Vit E (0.5:1.1, 0.5:2.3, 0.5:3.5, 0.5:4.7) and Ch to CEO-Vit E (0.5:2.4, 0.5:4.9, 0.5:7.4, 0.5:9.9) was also studied in the optimum ratio of Ch to TPP. The stability of resulted colloids was monitored during storage at 25 °C.

Characterization of NPs

The morphology and size of the colloidal NPs were characterized using a transmission electron microscope (TEM, JEOL 1230, Japan) at 100 kV after deposition onto a carbon-coated copper grid and air-drying. The freeze-dried NPs were also analyzed using a field-emission scanning electron microscope (FE-SEM, FEI Quanta 200, USA) at an accelerating voltage of 15 kV after deposition onto the sample holder and coating with a gold nanolayer using a Sputter Coater. The stability of colloidal NPs was initially assessed by the monitoring of their sedimentation over time. The hydrodynamic size distribution and zeta potential of NPs were also measured using a Zetasizer (ZEN 3600, Malvern, UK). Fourier transform infrared (FTIR, JASCO FT/IR-6300 spectrometer, Japan) spectroscopy was used to analyze the surface functional groups of the powdered samples. For this purpose, the dried samples were mixed with KBr powder and compressed into pellets and the spectra of the samples were recorded in the wavenumber range of 400–4000 cm^{-1}.

Antioxidant activity assays

The antioxidant activity of ChNPs, CEO ChNPs, Vit E ChNPs and CEO-Vit E ChNPs as well as CO, Vit E and CEO-Vit E emulsions was determined by the ABTS and DPPH free radical scavenging assays, based on the previous reports[25,29]. For DPPH assay, different volumes (10, 20, 40, 60, 80, 100 µL) of each sample was mixed with ethanolic solution of DPPH (0.1 mM, 1 mL) and incubated at ambient temperature in the dark for 1 h. The absorbance of samples was then measured at 517 nm using a UV-Vis spectrophotometer (HP-8453, UV–Vis, USA). A control sample was also prepared without CEO-Vit E particles and ethanol was used for the baseline correction. The antioxidant capacity was determined as a percentage of DPPH radical scavenging capacity of samples using the following formula:

$$\text{Radical scavenging activity } (\%) = [(A_{control} - A_{sample})/A_{control}] \times 100$$

Where, $A_{control}$ and A_{sample} are the absorbances of control and sample, respectively.

For ABTS assay, the stock solutions of ABTS (7 mM) and potassium persulfate (2.45 mM) were first prepared in the ultrapure water. The ABTS radical ($ABTS^{\bullet}$) solution was prepared by the addition of potassium persulfate solution (final concentration of 2.45 mM) to the ABTS solution and overnight incubation at room temperature in the dark. The $ABTS^{\bullet}$ solution was then diluted with distilled water until its optical density (OD) reached 0.7. Then, different volumes (10, 20, 40, 60, 80, 100 µL) of each sample were mixed with 800 µL of diluted $ABTS^{\bullet}$ solution and incubated at ambient temperature in the dark for 6 min. The absorbance of solutions was then measured at 734 nm using a UV-Vis spectrophotometer (HP-8453, UV–vis, USA). A control sample was also prepared without using the NPs and the ultra-pure water was used for the baseline correction. The antioxidant capacity was determined as percentage of ABTS radical scavenging activity using the following formula:

$$\text{Radical scavenging activity } (\%) = [(A_{control} - A_{sample})/A_{control}] \times 100$$

Where, $A_{control}$ and A_{sample} are the absorbances of control and target samples, respectively.

In vitro cell studies

The antibacterial effects of samples were investigated by the agar well diffusion method, based on the previously reported method[30] with some modifications. Briefly, two bacterial strains of *S. aureus* (gram-positive) and *E. coli* (gram-negative) were first cultured in the nutrient broth medium for 24 h at 30 °C and 37 °C, respectively. The bacterial culture turbidity was subsequently adjusted to 0.5 McFarland standard and spread on the Mueller Hinton agar plates. Then, 100 µL of each sample or the reference antibiotics (amoxicillin and gentamicin) were added into the as-prepared 5 mm holes on the plates. Finally, the inhibition zone (IZ) of each hole was measured after 18 h incubation at the appropriate temperature.

The minimum inhibitory concentration (MIC) and minimum bactericidal concentration (MBC) of the samples were also determined using the broth microdilution method, based on the recently published article[31]. Briefly, 100 µL of the bacterial culture with 0.5 McFarland standard turbidity in the sterile Mueller Hinton broth medium was added into each well of 96-well microtiter plate. A serial dilution of each sample was also prepared using the sterile deionized water and added (100 µL) into the individual wells. The bacterial suspension without sample was used as the negative control. MIC values were determined by measuring OD of the individual wells at 630 nm after 18 h incubation using a microplate reader (Agilent 800TS microplate reader, USA).

The potential antifungal activity of samples was studied on *A. niger* by the pour plate method, based on the previous report[32] with some modifications. For this purpose, different concentrations (0, 10, 20, and 50 mg mL^{-1}) of the samples were individually mixed with the sterilized PDA plates and solidified. 5 mm mycelium discs were then excised from the periphery of *A. niger* plates using a sterile scalpel and placed in the center of PDA plates and sealed with parafilm. The plates were incubated at 25 °C for 5–7 days, until the growth of mycelium in the control group reached the edges of the plates. Each experiment was conducted in triplicate, and the antifungal index for each treatment was calculated using the following formula:

$$\text{ntifungal index } (\%) = ((C - T)/C)*100.$$

Where C and T are the radial growth (mm) of mycelia in the control and treated plates, respectively.

The potential cytotoxicity of NPs was also evaluated on the human fibroblast cells using the MTT assay, based on the previous report[33]. Briefly, the cells were seeded at a density of 10^4 cells per well in a 96-well plate and incubated for 24 h at 37 °C in a humidified incubator with 5% CO_2. After cell adhesion and initial growth, various concentrations of ChNPs and CEO ChNPs (12.5, 25, 50, 100, and 200 µg mL^{-1}) were added into the individual wells and incubated under the same condition for 24 h. The culture medium was then completely removed and 100 µL of MTT solution (0.5 mg mL^{-1} in culture medium) was added into each well and incubated again for 4 h under the same condition. The medium was then carefully removed and 100 µL DMSO was added into the wells and incubated for 5 min to dissolve the formazan crystals. Then, OD of wells was measured at 570 nm, and the percentage of cell viability was calculated as the ratio of the OD of each treatment to the control. Results were expressed as the mean ± standard deviation (SD) of three independent experiments.

Molecular docking studies

Three-dimensional (3D) structures of eugenol and α-tocopherol were obtained from the PubChem database, and the 3D structure of Ch was retrieved from Figshare. The microbial target proteins were selected from the RCSB Protein Data Bank (RCSB PDB), based on their critical roles in microbial viability and pathogenicity. DNA gyrase (PDB ID: 1AB4), dihydrofolate reductase (DHFR, PDB ID: 1RA3), and MurA (PDB ID: 1UAE) were selected from *Escherichia coli*. DNA gyrase is an essential type II topoisomerase responsible for negative supercoiling of DNA during replication and transcription. DHFR is a key target protein in the bacterial infection therapy due to its central role in folate metabolism and nucleotide biosynthesis. MurA is a key enzyme in the early stage of peptidoglycan biosynthesis and thus, is essential for bacterial cell wall formation. Penicillin-binding protein 2a (PBP2a, PDB ID: 1MTW), Sortase A (PDB ID: 1T2W), and DNA gyrase (PDB ID: 2XCT) were selected from *Staphylococcus aureus*. PBP2a is responsible for cell wall crosslinking and is associated with β-lactam antibiotic resistance. Sortase A is a membrane-anchored enzyme involved in anchoring virulence-associated proteins to the bacterial surface, facilitating adhesion and immune evasion. Due to the unavailability of lanosterol synthase structure from *Aspergillus niger*, the homologous enzyme from *A. fumigatus* (PDB ID: 4UYM) was selected. This enzyme catalyzes a critical step in ergosterol biosynthesis, a key component of fungal membranes.

The protein structures were prepared using UCSF Chimera v1.19 for water removal, polar hydrogen addition, and energy minimization. Ligand preparation and charge assignment were conducted using AutoDock Tools (ADT) with Kollman charges. Docking simulations were performed via the HDOCK web server, which automatically generates 100 binding poses per ligand–receptor pair and ranks them based on predicted docking energy. Docking was performed on the full hexamer without fragmenting or averaging scores across repeating units. The single top-ranked pose for each protein–ligand pair was selected, and the corresponding docking score reported. The top 10 ranked poses were retrieved, and the best-scoring pose (rank 1) was selected as the representative binding model for further visualization and interaction analysis using the Protein–Ligand Interaction Profiler (PLIP) server.

Statistical analysis

One-way analysis of variance (ANOVA) was utilized for a completely randomized statistical analysis. Tukey's multiple comparison test was also applied at a significance level of $P < 0.05$ to determine the significant differences among means. The SPSS software (version 23.0) was used for the statistical analyses. All the antioxidant assays (section "Antioxidant activity assays") and in vitro cell studies (section "In vitro cell studies") were performed in triplicate and the results were expressed as the mean value ± SD of three independent experiments.

Results and discussion

Synthesis of ChNPs and their loading with CEO and Vit E

The effect of different ratios of Ch to TPP on the synthesis of ChNPs was investigated by monitoring of the absorbance wavelength (200 to 600 nm) of the reaction mixtures at specific time intervals over 60 min using a UV-Vis spectrophotometer (HP/Agilent 8453, USA). The results (Fig. 1a) showed the appearance of a prominent absorption peak at 236 nm, which is the characteristic wavelength of ChNPs[25], indicating the successful synthesis of ChNPs. The absorbance spectra also clearly showed a fast reaction kinetics during the first few minutes. Moreover, a more intense absorption peak was observed at 236 nm by increasing of the Ch concentration that

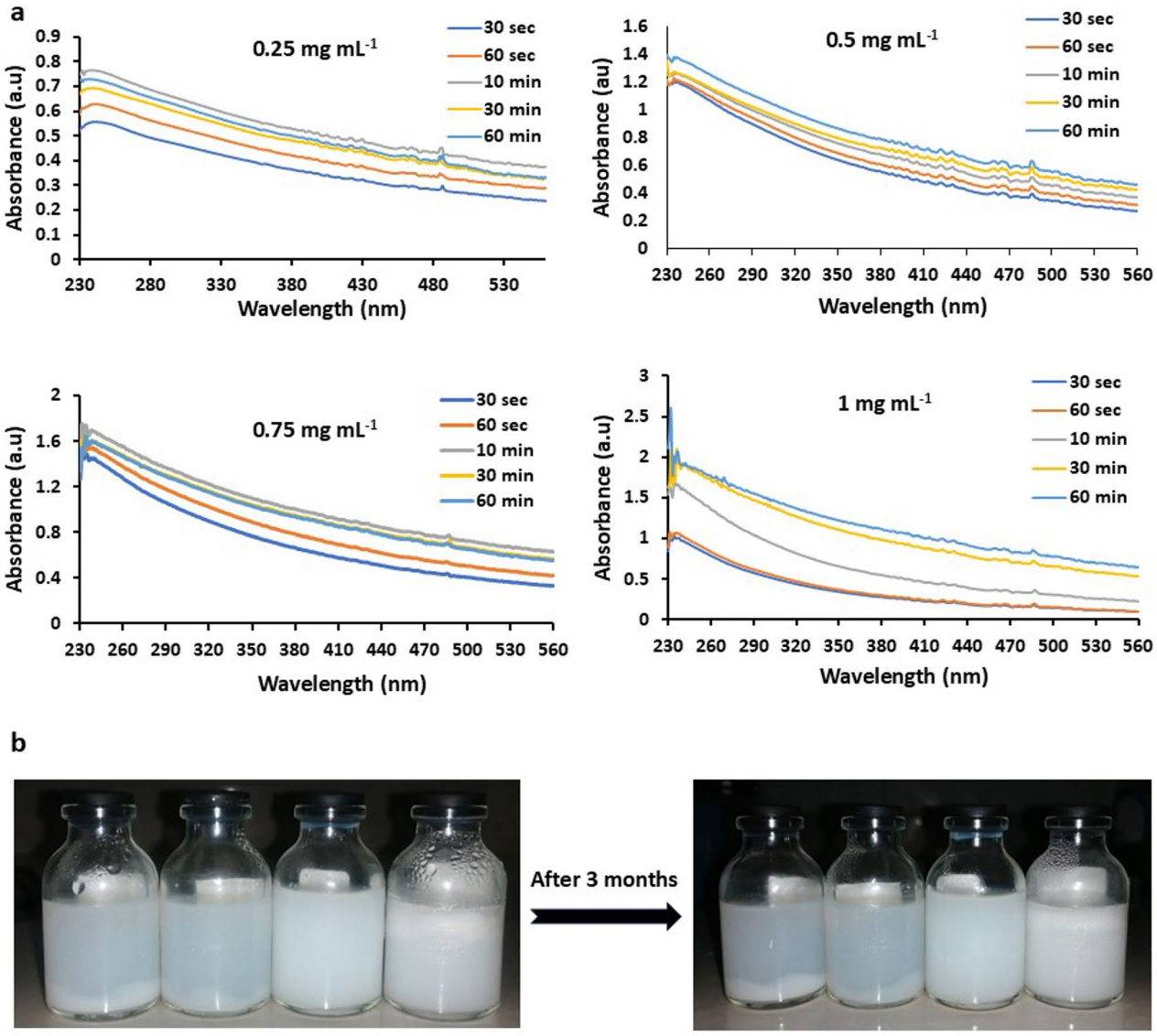

Fig. 1. Monitoring of the absorbance spectra of synthesized ChNPs at specific time intervals over 60 min (a), and the colloidal stability of synthesized CEO-Vit E ChNPs with different concentrations (left to right: 2.4, 4.9, 7.4 and 9.9 mg mL^{-1}) of CEO and Vit E (b).

indicates the synthesis of more NPs. This observation was also confirmed by measuring of the dry weight of ChNPs after centrifugation and freeze drying of the colloids (Table S1). However, the colloidal stability of ChNPs decreased significantly in the higher concentration of Ch, leading to their rapid precipitation. Based on the results, Ch toTPP ratio of 0.5:1 was chosen as the optimum ratio for further studies.

In the next step, different concentrations of CEO and Vit E with the equal ratios (1:1) were loaded into ChNPs, and the colloidal stability of resulted NPs was evaluated to determine the optimum condition. The results (Table S2) showed the significant effect of oil concentration on the colloidal stability of NPs over time. Based on the results, a final concentration of 7.4 mg mL^{-1} oil phase (75 µL CEO and 75 µL Vit E in total reaction volume of 20 mL) and Ch to TPP ratio of 0.5 to 1 mg mL^{-1}, respectively, was selected as the optimum condition for synthesis of stable CEO-Vit E ChNPs. The resulted colloids remained stable more than three months at 4 °C, without the significant creaming or sedimentation (Fig. 1b).

Characterization of CEO-Vit E ChNPs

The average hydrodynamic sizes of ChNPs and CEO-Vit E ChNPs were first measured using dynamic light scattering (DLS) instrument. The results showed significant increase of the hydrodynamic size of ChNPs from 198.1 nm to 306.6 nm (Fig. S1), following the incorporation of oil phase that is in consistent with the previous reports[27,34]. Hosseini et al.[27] similarly reported an increase in the average size of ChNPs from 281.5 nm to 309.8-402.2 nm after loading with the oregano EO. However, they also used CH_2Cl_2 and Tween 80 in the synthesis of

ChNPs, which are toxic and unsuitable for the biomedical and food applications. Interestingly, we succeeded to synthesize stable ChNPs loaded with CEO and Vit E without using any surfactants.

The resulted CEO-Vit E ChNPs also represented a polydispersity index of 0.387, indicating their relatively uniform size distribution. This result was also in accordance with the results of TEM analysis (Fig. 2a) that reveled the synthesis of semi-spherical, uniform and monodisperse ChNPs with the sizes of less than 50 nm. However, our attempt to achieve high-quality FE-SEM images of CEO-Vit E ChNPs failed (Fig. S2), mainly due to the presence of CEO that interfere with the complete drying of the samples. The obvious difference observed between the actual size of ChNPs and their hydrodynamic sixe could be attributed to the significant hydration layer surrounding the ChNPs. The thick hydration layer is responsible for high colloidal stability of NPs which is also consistent with the visual observations. The resulted CEO-Vit E ChNPs also represented a zeta potential value of −17 mV (Fig. S3) that indicates high negative surface charge of ChNPs. Similarly, the negative zeta potential values of up to −21.12 mV and − 23.1 mV were reported for ChNPs loaded with *Satureja hortensis* L.[35] and turmeric EOs[36], respectively. This significant negative charge that is mainly attributed to the carbonyl, hydroxyl, and carboxyl functional groups on the surface of ChNPs, plays a crucial role in their colloidal stability and prevents their agglomeration and subsequent precipitation.

The FTIR spectra of ChNPs, CEO ChNPs, Vit E ChNPs, and CEO-Vit E ChNPs are presented in Fig. 2b. The FTIR spectrum of ChNPs contains outstanding peaks at 3445 cm^{-1} (O–H), 3298 cm^{-1} (N–H2 stretching), 2991 cm^{-1} (C–H stretching), 1546 cm^{-1} (N–H_2 of amide II), 1367 cm^{-1} (C–N stretching), 1201 cm^{-1} (β-(1 – 4) glycosidic linkage), 1065 cm^{-1} (C–O–C stretching in the glucose ring), 997 cm^{-1} (C–O stretching), and 904 cm^{-1} (vibration of the pyranose ring)[37]. The peaks at 1065 cm^{-1} (C–O–C stretching in the glucose ring) and 1546 cm^{-1} (amide II) also suggest the electrostatic interactions between the PO_4^{3-} group of TPP and the NH_3^+ group of Ch[27,28]. The outstanding peaks located at 2732 cm^{-1}, 2672 cm^{-1}, and 2599 cm^{-1} in the FTIR spectrum of Vit E are corresponding to C–O–OH, N–H_2 and C–H stretching, respectively, while peak at 1100 cm^{-1} is attributed to the C–O stretching[38,39].

Antioxidant activity measurement

Regarding the well-known antioxidant activity of Vit E[40] and CEO[2]studying the effects of encapsulation on their antioxidant properties is appropriate. For this purpose, both free and encapsulated forms of CEO and Vit E were evaluated by the well-known ABTS and DPPH methods. The results (Fig. 3) showed a concentration-dependent antioxidant activity of the compounds. Based on the results, CEO and CEO-Vit E emulsions represented higher antioxidant activities than Vit E emulsion. Interestingly, the antioxidant activity of compounds increased after their encapsulation in ChNPs. ABTS assay revealed that the antioxidant activities of Vit E, CEO, and CEO-Vit E emulsions in the concentration of 2000 μg mL^{-1} increased from 36.84, 55.97, and 46.21% to 43.37, 75.66, and 59.42%, respectively, after Ch encapsulation (Fig. 3). The antioxidant activity of 98.34% also obtained for the equal concentration of ascorbic acid. The results were also confirmed by the DPPH assay. The results clearly showed the comparable antioxidant activity of CEO ChNPs with the control (ascorbic acid). In contrast, ChNPs showed the lowest antioxidant activity with 30.87% at the same concentration. Recently, the similar results have also been reported by Đorđević et al. regarding the improved antioxidant activity of *Ocimum basilicum* L. and *Satureja montana* L. EOs after Ch encapsulation[41]. Similar results have also been reported by Xie et al. for the Pickering emulsions of peppermint oil stabilized by resveratrol-grafted zein covalent conjugate/quaternary ammonium Ch[42]. However, no synergistic effect was observed following the co-loading of CEO and VitE that could be attributed to the masking effect due to the interaction between Vit E and CEO constitutes[43]. Another interesting result was the improved antioxidant activity of Vit E ChNPs over time. According to the results (Fig. S4), while the antioxidant activity of Vit E increased slightly (from 37.2 to 43.5%) over 48 h, the antioxidant activity of Vit E ChNPs significantly increased from 36.2 to 77.7%. This result can be attributed to the improved stability and gradual release of Vit E following Ch encapsulation. The high surface area to volume ratio of ChNPs, led to the increased bioavailability of hydrophobic CEO and thus, its higher biological activity[3].

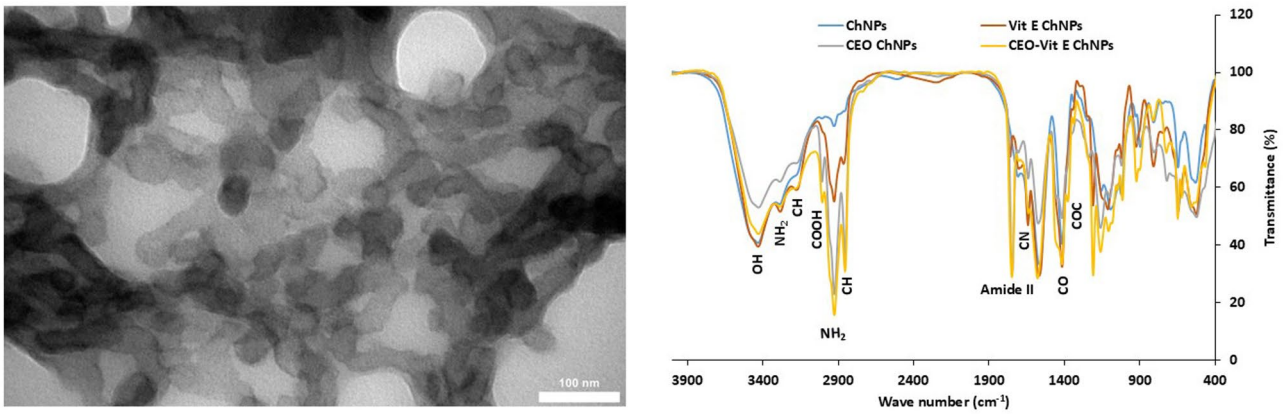

Fig. 2. TEM image of CEO-Vit E ChNPs (left) and FTIR spectra of ChNPs, CEO ChNPs, Vit E ChNPs, and CEO-Vit E ChNPs loaded with CEO, Vit E, and CEO-Vit E combination (right).

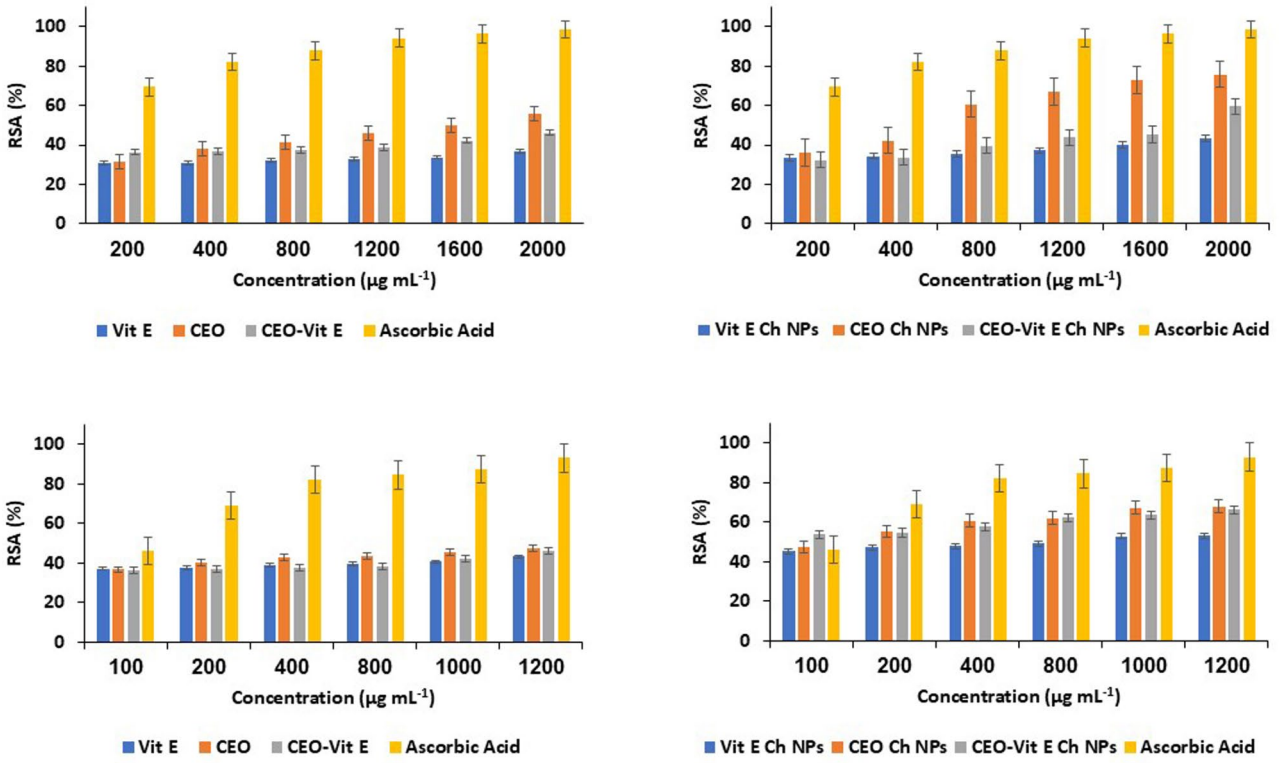

Fig. 3. The antioxidant activity of different concentrations of CEO, Vit E, and CEO-Vit E emulsions before (left) and after (right) encapsulation in ChNPs by ABTS (up) and DPPH (down) methods. The corresponding concentrations of ascorbic acid were used as the control.

In vitro cell studies

The antibacterial activity of ChNPs, CEO ChNPs, Vit E ChNPs, and CEO-Vit E ChNPs was first studied on *S. aureus* and *E. coli* strains using the agar well diffusion method. The results (Fig. 4a) indicated that ChNPs exhibited the highest antibacterial activity on *S. aureus*, with an average IZ of 18.1 mm in the final concentration of 0.5 mg mL^{-1}, while IZ of 19.4 mm was obtained for the same concentration of the antibiotic amoxicillin. The obtained IZs for CEO ChNPs, CEO-Vit E ChNPs, and Vit E ChNPs include 16.9, 16.1, and 14.5 mm (Table 1). The results of well diffusion method also indicated that the antibacterial effects of these NPs on *E. coli* were lower than those observed against *S. aureus* that could be attributed to the complex cell wall structure of gram-negative *E. coli* and thus, its lower permeability to the NPs[31].

The antibacterial activity of the samples was further evaluated on *S. aureus* and *E. coli* using the microbroth dilution method. The results (Table 1), in accordance with the results of agar well diffusion method, showed the higher antibacterial activity of samples on *S. aureus* than *E. coli*. Similarly, ChNPs and CEO ChNPs represented the highest antibacterial activity on *S. aureus* with the MIC value of 152 and 550 μg mL^{-1} while the MIC values of 987.5 and 1000 μg mL^{-1} obtained for Vit E ChNPs and CEO-Vit E ChNPs, respectively. Moreover, MBC values of 250, 1200, and 3950 μg mL^{-1} obtained for ChNPs, CEO ChNPs and CEO-Vit E ChNPs, respectively, while none of the tested concentrations of Vit E ChNPs caused complete bacterial death. The CEO loading of ChNPs led to the reduction of MIC from 975 to 550 μg mL^{-1} and also reduction of MBC from 1950 to 1200 μg mL^{-1}. Therefore, the encapsulation of CEO in ChNPs enhanced its antibacterial efficacy. This observation can be attributed to the increased stability and bioavailability of CEO after Ch encapsulation. Moreover, Ch can enhance the permeability of bacterial cell membranes[44] and thus, increase the penetration efficiency of EOs. On the other hand, Ch encapsulation can lead to the controlled and sustained release of EOs, ensuring a prolonged antibacterial effect[45].

The antifungal index of different concentrations of CEO ChNPs against *A. Niger* is presented in Fig. S5. The growth inhibition of *A. Niger* discs on the PDA media containing different concentrations of CEO ChNPs is also presented in Fig. 4b. The results clearly indicate the concentration-dependent antifungal activity of the samples such that the complete growth inhibition of fungal mycelial was achieved at 50 mg mL^{-1} of CEO ChNPs. This results are in accordance with the results reported by Hasheminejad et al.[46], regarding the complete inhibition of the mycelial growth of *A. niger* by the CEO encapsulated ChNPs. Since the using of high concentrations of EOs can negatively affect the smell and taste of food products, the encapsulation of EOs can reduce their concentration in the food products and, as a result, mitigate the related problems[47,48]. The higher antifungal against *Aspergillus flavus* and antiviral effects against human immunodeficiency virus type 1 were also reported previously through the nano-encapsulation of *Mentha piperita* EO and foscarnet[49,50]. Furthermore, Jose et al.[51]

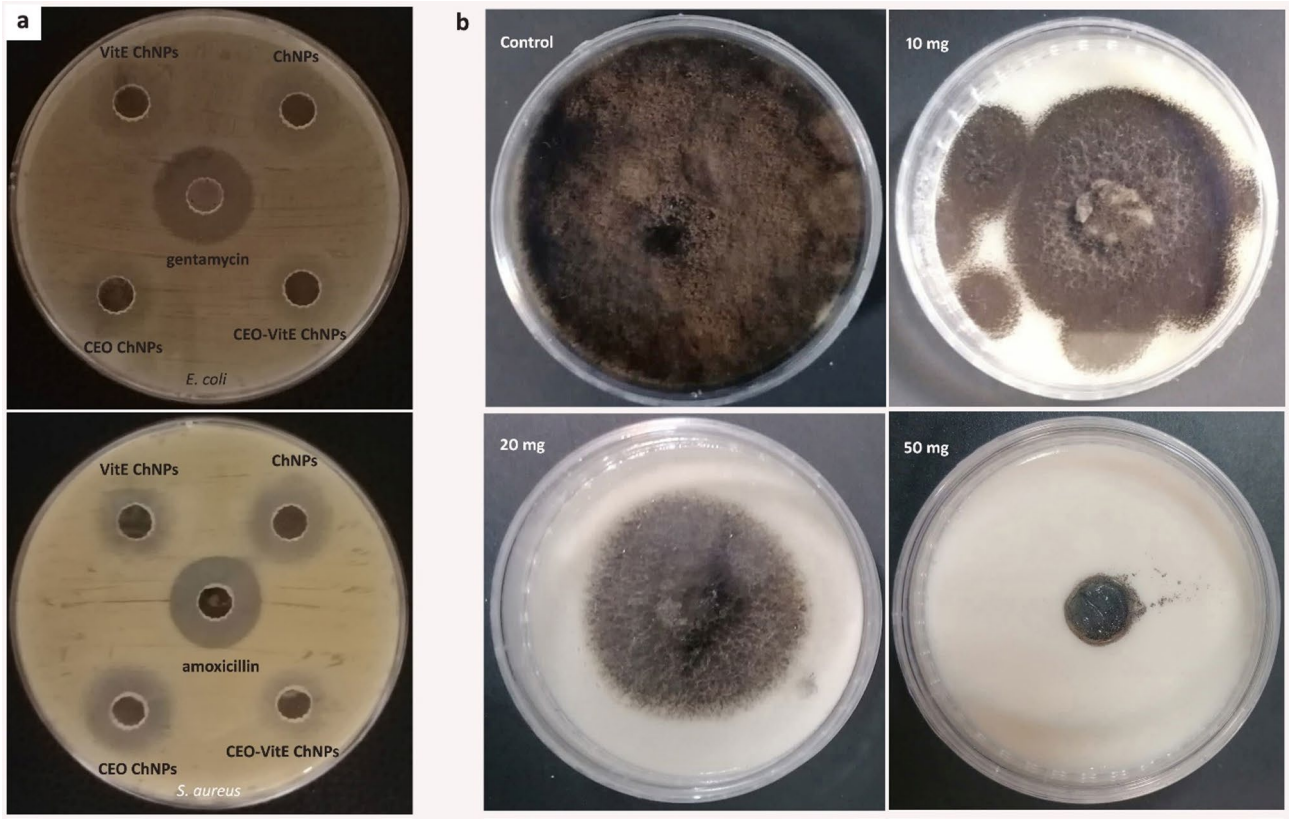

Fig. 4. Agar well difussion assay of ChNPs, Vit E ChNPs, CEO ChNPs, CEO-Vit E ChNPs and the coresponding antibiotic (gentamycin and amoxicillin) on *E. coli* and *S. aureus* (a). Antifungal activity of different concentrations (0, 10, 20, and 50 mg mL^{1}) of CEO ChNPs against *A. niger* (b).

Antibacterial activity	*E. coli*			*S. aureus*		
	IZ (mm)	MIC (μg mL^{-1})	MBC (μg mL^{-1})	IZ (mm)	MIC (μg mL^{-1})	MBC (μg mL^{-1})
ChNPs	14.5	250	---	18.1	152	250
Vit E ChNPs	13.9	1750	---	14.5	1000	---
CEO ChNPs	13.6	1200	---	16.9	550	1200
CEO-Vit E ChNPs	14.1	3700	---	16.1	987.5	3950
Antibiotic	18.5	---	---	19.4	---	---

Table 1. IZ, MIC, and MBC values of chnps, Vit E chnps, CEO chnps, CEO-Vit E ChNPs and (F) the coresponding antibiotic (gentamycin and amoxicillin) on *E. coli* and *S. aureus*.

reported the potent antifungal activity of polyvinyl alcohol nanocomposites integrated with CEO and ChNPs against *Pythium aphanidermatum*. This study suggests the potential applications of Ch-based nano-formulations in antimicrobial coatings and biomedical fields.

Given the importance and necessity of biocompatibility and the absence of harmful toxic effects of food ingredients, including the additives and preservatives, the potential cytotoxicity of NPs was also preliminary investigated using the MTT assay. Certainly, a complete understanding of the effects of nano-formulations requires an extensive and complete study on their biocompatibility, anti-cancer effects, anti-inflammatory activity, and wound healing properties in vitro and in vivo, which will be addressed in subsequent studies. Interestingly, the results (Fig. S6) showed that the CEO and Vit E loading led to the improved biocompatibility of ChNPs. While only 35.61% of the cells remained viable after 24 h exposure with 200 μg mL^{-1} ChNPs, the cell viabilities of 72.84% and 81.73% were observed using CEO ChNPs and CEO-Vit E ChNPs, at the same condition. The results indicate that the resulted nano-formulation does not exhibit toxicity toward human cells, making it appropriate for a variety of biomedical and food applications. The improved biocompatibility of ChNPs could be mainly attributed to the well-known antioxidant activity of CEO and Vit E[52,53], which reduces the potential oxidative stress and inflammation of ChNPs.

Target Protein	PDB ID	Microorganism	Ligand	Number of H-Bonds	HDOCK Score (arb. units)
DNA gyrase	1AB4	*E. coli*	Ch	14	−226.36
			Eugenol	2	−93.21
			Vit E	3	−134.78
DHFR	1RA3	*E. coli*	Ch	9	−191.82
			Eugenol	4	−87.38
			Vit E	4	−136.21
MURA	1UAE	*E. coli*	Ch	3	−203.85
			Eugenol	1	−96.06
			Vit E	4	−125.57
PBP2a	1MTW	*S. aureus*	Ch	16	−238.43
			Eugenol	3	−98.50
			Vit E	7	−136.87
Sortase	1T2W	*S. aureus*	Ch	17	−254.97
			Eugenol	4	−102.13
			Vit E	7	−138.04
DNA gyrase	2XCT	*S. aureus*	Ch	22	−343.58
			Eugenol	21	−134.22
			Vit E	18	−207.34
Lanosterol	4UYM	*A. fumigatus*	Ch	11	−240.25
			Eugenol	6	−104.25
			Vit E	11	−173.11

Table 2. Molecular Docking results of ch, eugenol, and Vit E against different microbial proteins. Docking scores are from the HDOCK server (arbitrary units; more negative values indicate stronger predicted binding).

Recently, Suflet et al.[54] have also reported the low toxicity of CEO loaded Ch–oxidized pullulan hydrogels that further confirm the high potential of ChNPs as a carrier for delivering of the natural compounds. Yadav et al. have also reviewed the high potential of Ch-based nano-formulations for drug delivery and therapeutic applications with emphasis on their high biocompatibility[55]. Sharma et al. have also reported recently, the non-toxic nature of Ch nanocomposites and their suitability for the biomedical applications[56]. Ch was also reported by Detsi et al. as an excellent biopolymer matrix for encapsulation of the natural products with low toxicity[57].

Molecular docking

The computational methods are commonly used to predict the interaction of natural substances with the bacterial targets, such as DNA gyrase, DHFR, and PBP[58,59]. Therefore, the molecular docking was used to better understand the molecular action mechanisms of Ch, eugenol, and Vit E on *E. coli*, *S. aureus*, and *A. niger*. Docking simulations were performed using the HDOCK server, which applies a hybrid strategy combining template-based modelling and ab initio docking. This platform was used because it supports large and flexible ligands, such as Ch hexamer, without requiring extensive manual preprocessing or fragmentation. This server integrates both template-based and template-free docking, making it suitable for targets with the limited co-crystallized ligand data, such as *A. fumigatus* lanosterol synthase. Moreover, the application of a single docking engine for all ligand-target pairs could ensure the comparability of results. In the simulations, Ch was modelled as a hexamer consisting of six β-(1→4)-linked D-glucosamine units, with fully protonated amino groups to reflect its cationic nature at the physiological pH. This oligomer length has been widely employed for the in silico Ch research[60], because it retains the essential interaction features of the polymer while remaining computationally tractable. Importantly, the 3D structure of Ch hexamer used in this study was obtained from the Figshare repository, where pre-constructed and validated Ch oligomer models are publicly available. This ensures the reliability and reproducibility of the ligand structure, avoiding potential biases or inaccuracies from *de novo* modeling. For each protein–ligand pair, the top-ranked pose predicted by HDOCK was selected for further analysis.

The obtained 3D images by the Protein-Ligand Interaction Profiler web tool showed the interaction of ligands (Ch, eugenol, and α-tocopherol) with different target proteins of *E. coli* (Fig. S7), *S. aureus* (Fig. S8) and *A. fumigatus* (Fig. S9). The numerical values reported in Table 2 represent HDOCK docking scores, which are calculated from a knowledge-based statistical potential combined with shape complementarity, rather than direct thermodynamic free energies (ΔG) in kcal·mol^{-1}. Although such scores are sometimes referred to as "binding energies" for simplicity, they are expressed in arbitrary units and should be interpreted only in a relative sense: more negative values indicate stronger predicted binding compared to other ligands docked to the same target under identical conditions. The significant reduction was observed in the calculated HDOCK docking scores following the interaction of the ligands with the bacterial and fungal proteins (Table 2), indicating high affinity of the ligands to the targeted proteins. These observations revealed that Ch, eugenol, and α-tocopherol can bind to different bacterial and fungal proteins and thus, affect their function and viability of cells. The docking results (Table 2) showed that Ch consistently achieved the most negative scores and formed the largest number of hydrogen bonds with the target proteins, particularly *S. aureus* DNA gyrase (−343.58), Sortase (−254.97), and *A.*

fumigatus lanosterol synthase (−240.25). These strong predicted interactions suggest the potential interference with the critical microbial processes, such as DNA replication, protein anchoring to the cell wall, and membrane biosynthesis. In contrast, eugenol and VitE exhibited less negative docking scores and fewer hydrogen bonds, which aligns with their lower direct antimicrobial activity observed in vitro. Notably, encapsulation of eugenol and VitE in ChNPs enhanced their antimicrobial activity, likely due to the Ch-mediated facilitation of cellular uptake and improved accessibility to intracellular targets.

Although Vit E showed strong docking scores (e.g., − 173.11 kcal mol^{-1} with lanosterol synthase), no similar performance was observed in vitro, likely due to its poor water solubility and limited bioavailability in the physiological environment. Since 3D structure of lanosterol synthase has not been reported for *Aspergillus niger* until now, the 3D structure of *A. fumigatus* enzyme (PDB ID: 4UYM) was used as a target for molecular docking. Similarly, Ch represented strongest binding (−240.25 kcal mol^{-1}) to *A. fumigatus* lanosterol synthase, followed by Vit E (−173.11 kcal mol^{-1}) and eugenol (−104.25 kcal mol^{-1}), reflecting the same ranking observed in antibacterial docking. Overall, the docking simulations support the experimental findings by suggesting that Ch can strongly interact with multiple microbial proteins, potentially disrupting their biological function, while also serving as an effective carrier to enhance the activity of co-encapsulated bioactive compounds.

Conclusion

Despite the unique biological properties of Vit E and plant EOs, their high hydrophobicity and volatility have severely limited their applications. Encapsulation of these compounds with biopolymers such as Ch is an effective strategy to solve this problem. In addition, the well-known antimicrobial activity of Ch may represent the synergistic effects, leading to achievement of new formulations with superior biological properties. Moreover, the multifunctional nano-formulations with diverse biological properties can be developed by using different compounds and also by the modification of physicochemical characteristics of ChNPs. The results of present study demonstrated high potential of ChNPs as nanocarriers for development of such multifunctional nano-formulations with the antioxidant, antibacterial and antifungal effects. This significant bioactivity can be attributed to the better dispersion, increased surface area, and controlled release of ingredients. The enhanced antibacterial activity may also stem from the electrostatic attraction of positively charged Ch and bacterial cell membranes, which disrupts membrane integrity and boosts the bioavailability of active compounds. Regarding the results of computational studies that revealed strongest bonding of Ch to the target proteins, it can be concluded that co-delivery of EOs and Vit E in ChNPs enhances the bioactivity, solubility, membrane disruption, and cellular uptake of compounds, possibly through the synergistic effects. Given the high nutritional value of plant EOs, especially CEO, their combination with Vit E can be used in the development of functional foods, which is very valuable in nutritional health. The antibacterial and anti-fungal properties of these compounds play a significant role not only in improving consumer health but also in the preservation and shelf life of the food products. Therefore, development of such delivery systems can be a very suitable alternative to chemical preservatives in food products. Moreover, investigating different combinations of these food additives to achieve superior and novel biological and pharmaceutical properties is an attractive field of research that can also improve human health. In this regard, the computational studies of the potential inter-molecular interactions can also be useful to select the appropriate combinations and to obtain the highest bioactivities.

Data availability

All data generated or analyzed during this study are included in this published article (and its Supplementary Information file).

Received: 29 May 2025; Accepted: 29 August 2025
Published online: 01 September 2025

References

1. Yammine, J., Chihib, N. E., Gharsallaoui, A., Ismail, A. & Karam, L. Advances in essential oils encapsulation: development, characterization and release mechanisms. *Polym. Bull.* **81**, 3837–3882 (2024).
2. Liñán-Atero, R. et al. Clove essential oil: chemical profile, biological activities, encapsulation strategies, and food applications. *Antioxidants* **13**, 1–38 (2024).
3. Xu, F. et al. Characterization, stability and antioxidant activity of vanilla Nano-Emulsion and its complex essential oil. *Foods* **13**, 801 (2024).
4. Hyldgaard, M., Mygind, T. & Meyer, R. L. Essential oils in food preservation: mode of action, synergies, and interactions with food matrix components. *Front. Microbiol.* **3**, 1–24 (2012).
5. da Silva, B. D., Bernardes, P. C., Pinheiro, P. F., Fantuzzi, E. & Roberto, C. D. Chemical composition, extraction sources and action mechanisms of essential oils: natural preservative and limitations of use in meat products. *Meat Sci.* **176**, 108463 (2021).
6. Silva, M. V. et al. R. G. C. da Silva, L. E. P. T. de Moraes Filho, I. D. de Lima Silva and Clove essential oil and eugenol: A review of their significance and uses. *Food Biosci.* **62**, 105112 (2024).
7. Lucia, A. & Guzmán, E. Emulsions containing essential oils, their components or volatile semiochemicals as promising tools for insect pest and pathogen management. *Adv Colloid Interface Sci.* **287** (2021).
8. Stoleru, E. & Brebu, M. Stabilization techniques of essential oils by incorporation into biodegradable polymeric materials for food packaging. *Molecules* **26**, 6307 (2021).
9. Lim, X. Y. et al. Stabilization of essential oil: Polysaccharide-Based drug delivery system with Plant-like structure based on biomimetic concept. *Polymers (Basel).* **15**, 3338 (2023).
10. Pandey, V. K. et al. Bioactive properties of clove (*Syzygium aromaticum*) essential oil nanoemulsion: A comprehensive review. *Heliyon* **10**, e22437 (2024).
11. Batiha, G. E. S. et al. *Syzygium aromaticum* L. (myrtaceae): Traditional uses, bioactive chemical constituents, pharmacological and toxicological activities. *Biomolecules* **10**, 202 (2020).
12. Nirmal, N. P. et al. A comprehensive review on clove (*Caryophyllus aromaticus* L.) essential oil and its significance in the formulation of edible coatings for potential food applications. *Front. Nutr.* **9**, 987674 (2022).

13. Ralla, T. et al. Over 100 years of vitamin E: an overview from synthesis and formulation to application in animal nutrition. *J. Anim. Physiol. Anim. Nutr. (Berl).* **108**, 646–663 (2024).
14. Jang, Y. & Kim, C. Y. The role of vitamin E isoforms and metabolites in cancer prevention: mechanistic insights into sphingolipid metabolism modulation. *Nutr* **16**, 1–20 (2024).
15. Mohamadyan, W., Yousefi, S. & Weisany, W. Development of edible nanoemulsions containing vitamin E using a low-energy method: evaluation of particle size and physicochemical properties for food and beverage applications. *Heliyon* **10**, e32415 (2024).
16. Yang, Y. & McClements, D. J. Encapsulation of vitamin E in edible emulsions fabricated using a natural surfactant. *Food Hydrocoll.* **30**, 712–720 (2013).
17. Siddiqui, S. A. et al. Encapsulation of bioactive compounds in foods for diabetics - sources, encapsulation technologies, market trends and future perspectives – A systematic review. *Food Bioprod. Process.* **147**, 277–303 (2024).
18. Hisham, F., Maziati Akmal, M. H., Ahmad, F., Ahmad, K. & Samat, N. Biopolymer chitosan: potential sources, extraction methods, and emerging applications. *Ain Shams Eng. J.* **15**, 102424 (2024).
19. Rajabi, H., Jafari, S. M., Rajabzadeh, G., Sarfarazi, M. & Sedaghati, S. Chitosan-gum Arabic complex nanocarriers for encapsulation of saffron bioactive components. *Colloids Surf. Physicochem Eng. Asp*. **578**, 123644 (2019).
20. Esmaeili, A. & Asgari, A. *In vitro* release and biological activities of *Carum copticum* essential oil (CEO) loaded chitosan nanoparticles. *Int. J. Biol. Macromol*. **81**, 283–290 (2015).
21. Farag, E. A. H., Baromh, M. Z., El-kalamwi, N. & Sherif, A. H. Vitamin E nanoparticles enhance performance and immune status of nile tilapia. *BMC Vet. Res*. **20**, 561 (2024).
22. Sherif, A. H., Khalil, R. H., Talaat, T. S., Baromh, M. Z. & Elnagar, M. A. Dietary nanocomposite of vitamin C and vitamin E enhanced the performance of nile tilapia. *Sci. Rep.* **14**, 1–11 (2024).
23. Lin, S. J. & Pascall, M. A. Incorporation of vitamin E into Chitosan and its effect on the film forming solution (viscosity and drying rate) and the solubility andthermal properties of the dried film. *Food Hydrocoll.* **35**, 78–84 (2014).
24. Otoni, C. G., Pontes, S. F. O., Medeiros, E. & Soares, N. D. F. F. Edible films from Methylcellulose and nanoemulsions of clove bud (*Syzygium aromaticum*) and oregano (*Origanum vulgare*) essential oils as shelf life extenders for sliced bread. *J. Agric. Food Chem.* **62**, 5214–5219 (2014).
25. Hadidi, M., Pouramin, S., Adinepour, F., Haghani, S. & Jafari, S. M. Chitosan nanoparticles loaded with clove essential oil: characterization, antioxidant and antibacterial activities. *Carbohydr. Polym*. **236**, 116075 (2020).
26. Campelo, M. S. et al. Clove essential oil encapsulated on nanocarrier based on polysaccharide: A strategy for the treatment of vaginal candidiasis. *Colloids Surf. Physicochem Eng. Asp*. **610**, 125732 (2021).
27. Hosseini, S. F., Zandi, M., Rezaei, M. & Farahmandghavi, F. Two-step method for encapsulation of oregano essential oil in Chitosan nanoparticles: preparation, characterization and *in vitro* release study. *Carbohydr. Polym*. **95**, 50–56 (2013).
28. Keawchaoon, L. & Yoksan, R. Preparation, characterization and *in vitro* release study of carvacrol-loaded Chitosan nanoparticles. *Colloids Surf. B Biointerfaces*. **84**, 163–171 (2011).
29. Teixeira, B. et al. European Pennyroyal (*Mentha pulegium*) from portugal: chemical composition of essential oil and antioxidant and antimicrobial properties of extracts and essential oil. *Ind. Crops Prod.* **36**, 81–87 (2012).
30. Yazgan, H. Antimicrobial activities of emulsion-based edible solutions incorporating lemon essential oil and sodium caseinate against some food-borne bacteria. *J. Food Sci. Technol.* **59**, 4695–4705 (2022).
31. Abbasi Kajani, A., Bordbar, A. K., Pouresmaeili, A. & Ayatollahi, M. Green and one-step synthesis of fluorescent carbon Dots with the significant antibacterial effects. *Iran. J. Sci.* 1–8. (2024).
32. Askarne, L. et al. In vitro and in vivo antifungal activity of several Moroccan plants against *Penicillium italicum*, the causal agent of citrus blue mold. *Crop Prot*. **40**, 53–58 (2012).
33. Abbasi Kajani, A. et al. Beyzavi, green and facile synthesis of highly photoluminescent multicolor carbon nanocrystals for cancer therapy and imaging. *ACS Appl. Bio Mater.* **1**, 1458–1467 (2018).
34. Yoksan, R., Jirawutthiwongchai, J. & Arpo, K. Encapsulation of ascorbyl palmitate in Chitosan nanoparticles by oil-in-water emulsion and ionic gelation processes. *Colloids Surf. B Biointerfaces*. **76**, 292–297 (2010).
35. Feyzioglu, G. C. & Tornuk, F. Development of Chitosan nanoparticles loaded with summer savory (*Satureja hortensis* L.) essential oil for antimicrobial and antioxidant delivery applications. *Lwt* **70**, 104–110 (2016).
36. Lertsutthiwong, P., Rojsitthisak, P. & Nimmannit, U. Preparation of turmeric oil-loaded chitosan-alginate biopolymeric nanocapsules. *Mater. Sci. Eng. C*. **29**, 856–860 (2009).
37. Jiang, X. et al. Chitosan nanoparticles loaded with *Eucommia ulmoides* seed essential oil: preparation, characterization, antioxidant and antibacterial properties. *Int. J. Biol. Macromol.* **257**, 2023–2024 (2024).
38. Fathi, M., Nasrabadi, M. N. & Varshosaz, J. Characteristics of vitamin E-loaded nanofibres from dextran. *Int. J. Food Prop.* **20**, 2665–2674 (2017).
39. Pang, W., Wu, J., Zhang, Q. & Li, G. Graphene oxide enhanced, radiation cross-linked, vitamin E stabilized oxidation resistant UHMWPE with high hardness and tensile properties. *RSC Adv.* **7**, 55536–55546 (2017).
40. Latib, F., Zafendi, M. A. I., Mohd, M. A. & Lazaldin The use of vitamin E in ocular health: bridging omics approaches with Tocopherol and Tocotrienol in the management of glaucoma. *Food Chem. Mol. Sci.* **9**, 100224 (2024).
41. Đorđević, N. et al. Nanoencapsulation of *Ocimum Basilicum* L. and *Satureja Montana* L. Essential oil mixtures: enhanced antimicrobial and antioxidant activity. *Antibiotics* **14**, 1–20 (2025).
42. Ren, G. et al. Improved antioxidant activity and delivery of peppermint oil Pickering emulsion stabilized by resveratrol-grafted Zein covalent conjugate/quaternary ammonium Chitosan nanoparticles. *Int. J. Biol. Macromol.* **253**, 9–10 (2023).
43. Arts, M. J. T. J. et al. Interactions between flavonoids and proteins: effect on the total antioxidant capacity. *J. Agric. Food Chem.* **50**, 1184–1187 (2002).
44. Tao, Y., Qian, L. H. & Xie, J. Effect of Chitosan on membrane permeability and cell morphology of *Pseudomonas aeruginosa* and *Staphyloccocus aureus*. *Carbohydr. Polym.* **86**, 969–974 (2011).
45. Mohammadi, A., Hosseini, S. M. & Hashemi, M. Emerging Chitosan nanoparticles loading-system boosted the antibacterial activity of *Cinnamomum zeylanicum* essential oil. *Ind. Crops Prod.* **155**, 112824 (2020).
46. Hasheminejad, N., Khodaiyan, F. & Safari, M. Improving the antifungal activity of clove essential oil encapsulated by Chitosan nanoparticles. *Food Chem.* **275**, 113–122 (2019).
47. Donsì, F., Annunziata, M., Sessa, M. & Ferrari, G. Nanoencapsulation of essential oils to enhance their antimicrobial activity in foods. *Lwt* **44**, 1908–1914 (2011).
48. Hsieh, P. C., Mau, J. L. & Huang, S. H. Antimicrobial effect of various combinations of plant extracts. *Food Microbiol.* **18**, 35–43 (2001).
49. Beyki, M. et al. Encapsulation of *Mentha Piperita* essential oils in chitosan-cinnamic acid nanogel with enhanced antimicrobial activity against *Aspergillus flavus*. *Ind. Crops Prod.* **54**, 310–319 (2014).
50. Russo, E. et al. Preparation, characterization and *in vitro* antiviral activity evaluation of foscarnet-chitosan nanoparticles. *Colloids Surf. B Biointerfaces*. **118**, 117–125 (2014).
51. Jose, A., Anitha Sasidharan, S., Chacko, C., Mukkumkal Jacob, D. & Edayileveettil Krishnankutty, R. Activity of clove oil and Chitosan nanoparticles incorporated PVA nanocomposite against *Pythium aphanidermatum*. *Appl. Biochem. Biotechnol.* **194**, 1442–1457 (2022).
52. Stojanović, N. M. et al. Essential oil constituents as anti-Inflammatory and neuroprotective agents: an insight through microglia modulation. *Int. J. Mol. Sci.* **25**, 5168 (2024).

53. Singh, U., Devaraj, S., Jialal, I., Vitamin, E. & Oxidative stress, and inflammation. *Annu. Rev. Nutr.* **25**, 151–174 (2005).
54. Suflet, D. M. et al. Chitosan–Oxidized Pullulan hydrogels loaded with essential clove oil: synthesis, characterization, antioxidant and antimicrobial properties. *Gels* **10**, 227 (2024).
55. Yadav, S. et al. Chitosan-Based nanoformulations: preclinical investigations, theranostic advancements, and clinical trial prospects for targeting diverse pathologies. *AAPS PharmSciTech*. **25**, 263 (2024).
56. Sharma, D. K., Pattnaik, G., Moharana, S. & Behera, A. Chitosan and their nanocomposites for biomedical applications. *Novel Bio-nanocompos. Biomed. Appl.* 291–292 (2024).
57. Detsi, A. et al. Nanosystems for the encapsulation of natural products: the case of Chitosan biopolymer as a matrix. *Pharmaceutics* **12**, 1–68 (2020).
58. Kitchen, D. B., Decornez, H., Furr, J. R. & Bajorath, J. Docking and scoring in virtual screening for drug discovery: methods and applications. *Nat. Rev. Drug Discov.* **3**, 935–949 (2004).
59. Yu, W. & MacKerell, A. D. Computer-Aided drug design methods. *Methods Mol. Biol.* **1520**, 85–106 (2017).
60. Rinaudo, M. Chitin and chitosan: properties and applications. *Prog Polym. Sci.* **31**, 603–632 (2006).

Acknowledgements
The financial support of the Research Council of University of Isfahan is gratefully acknowledged.

Author contributions
Davoud Mahmoudi: Formal analysis and writing of the manuscript.Abolghasem Abbasi Kajani: conception, design, analysis and writing of the manuscript.Mohammad Rabbani Khorasgani: conception and methodology.

Declarations

Competing interests
The authors declare no competing interests.

Additional information
Supplementary Information The online version contains supplementary material available at https://doi.org/10.1038/s41598-025-18135-2.

Correspondence and requests for materials should be addressed to A.A.K.